Chinese Chemical Letters 32 (2021) 3886–3889

Contents lists available at ScienceDirect

Chinese Chemical Letters

journal homepage: www.elsevier.com/locate/cclet

Communication

Aza-BODIPY based probe for photoacoustic imaging of $ONOO^-$ *in vivo*

Danghui Ma[a], Shumin Hou[a], Chaeeon Bae[d], Thanh Chung Pham[d], Songyi Lee[c,d,*], Xin Zhou[a,b,**]

[a] *Department of Chemistry, College of Chemistry and Chemical Engineering, Qingdao 266071, China*
[b] *Qingdao Cancer Institute, Qingdao University, Qingdao 266071, China*
[c] *Department of Chemistry, Pukyong National University, Busan 48513, Korea*
[d] *Industry 4.0 Convergence Bionics Engineering, Pukyong National University, Busan 48513, Korea*

ARTICLE INFO

Article history:
Received 16 March 2021
Revised 18 May 2021
Accepted 24 May 2021
Available online 1 June 2021

Keywords:
Photoacoustic
$ONOO^-$
Imaging
Aza-BODIPY
In vivo

ABSTRACT

The effective detecting $ONOO^-$ variations *in vivo* is of great importance to well understand the complex pathophysiological processes. We reported here a photoacoustic (PA) probe **AZB-1** for imaging $ONOO^-$ *in vivo*. **AZB-1** showed an originally strong photoacoustic signal at 660 nm. And its PA signal can be turned off by shutting the ICT effect caused by the conjugated electron withdrawing group at 2-position of the aza-BODIPY core. Moreover, the probe was successfully employed to imaging $ONOO^-$ variations in inflammatory mice models. Wisely utilized this strategy may serve as powerful platforms for the preparation of novel PA chemosensors.

As a typical reactive nitrogen specie, peroxynitrite ($ONOO^-$) has drew wide attention due to its unusually potent oxidizing ability and strongly nucleophilic character [1–5]. The normal endogenous $ONOO^-$ is essential for maintaining cellular processes. Its role has been clearly proved in a mass of biophysiological events, including signal transduction pathways, forming nitrotyrosine residues and nitro fatty acid [6–10]. In contrast, the abnormal high concentration of $ONOO^-$ is harmful for the normal growth of cells, leading to the emergence of various diseases, such as diabetes, Alzheimer's disease, cardiovascular disease, and neurodegenerative diseases [11–14]. Therefore, it is of great significance to develop powerful analysis method for detecting $ONOO^-$ levels in organisms, in order to better understand complex pathophysiological processes.

Recently, the fluorescent probes have made significant progress in detecting $ONOO^-$, due to their unique advantages of high temporal and spatial resolution, as well as high sensitivity [15,16]. Moreover, some of them have realized the nondestructive and real-time imaging $ONOO^-$ in living cells and *in vivo* [17–22]. However, a major challenge with these fluorescent probes is the low resolution of imaging depth less than 1 mm due to their limited tissue penetration, which hampered the further monitoring $ONOO^-$ *in vivo*. Alternatively, photoacoustic molecular imaging (PA) is an emerging non-invasive biological imaging and sensing technology based on photoacoustic effect [23]. When biological tissue is irradiated by laser, photosensitive substances in the tissue absorb laser energy, generate instantaneous thermal expansion, and then radiate ultrasonic waves and stimulate photoacoustic signals. Photoacoustic imaging technology has the advantages of strong optical absorption, high spatial resolution, high contrast, and the ability to image in deep tissue [24]. Moreover, as a non-ionizing radiation imaging technology, photoacoustic imaging showed considerable tissue safety [25–28]. For this reason, some PA probes have been developed for a variety of applications, such as cancer detection [29], arthritis imaging [30], metal ions detection [31,32], imaging of reducing agents [33,34] and reactive oxygen species [35]. Although numbers of PA probes have been reported, only a few examples regarding $ONOO^-$ photoacoustic probes have been achieved to data [36,37].

Herein, we reported a photoacoustic probe **AZB-1** based on an aza-BODIPY derivative for detecting $ONOO^-$. The probe showed a strongest absorption peak at 660 nm and gave a strong photoa-

* Corresponding author at: Department of Chemistry, Pukyong National University, Busan 48513, Korea.
** Corresponding author at: Department of Chemistry, College of Chemistry and Chemical Engineering, Qingdao 266071, China.
E-mail addresses: slee@pknu.ac.kr (S. Lee), zhouxin@qdu.edu.cn (X. Zhou).

https://doi.org/10.1016/j.cclet.2021.05.048
1001-8417/

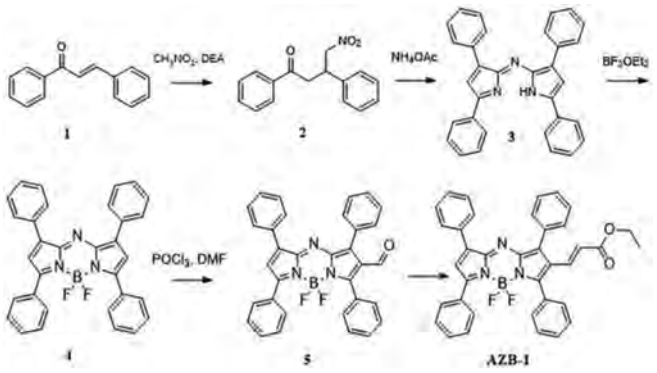

Scheme 1. Synthetic route of the probe **AZB-1**.

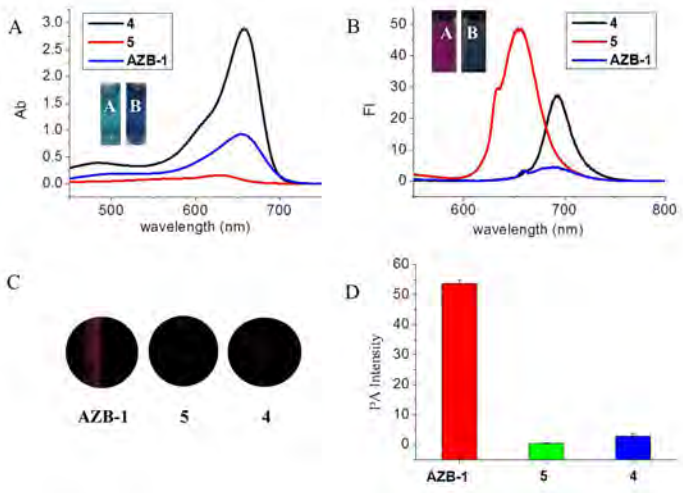

Fig. 1. (A) Absorption and (B) fluorescence spectra of the **AZB-1** (10 μmol/L), and its precursor **5** (10 μmol/L), and **4** (10 μmol/L), in DMSO solution. Inset: The color of the three compounds under natural light and UV lamp excited at 365 nm (A represents compound **5**, B represents **AZB-1**). (C) Photoacoustic signal of compounds **AZB-1, 5, 4**. (D) Photoacoustic signal value of **AZB-1, 5, 4**. The excitation wavelengths were 660 nm.

coustic signal. When reacted with $ONOO^-$, the conjugated group at 2-position of aza-BODIPY core can be readily oxidized, resulting in the shutting the ICT effect and the photoacoustic signal of the probe correspondingly. Wisely utilized this strategy may serve as powerful platforms for the preparation of novel photoacoustic chemosensors. Moreover, the probe was successfully employed to imaging $ONOO^-$ variations in inflammatory mice models.

To obtain an ideal probe with initial strong photoacoustic signal, tetraphenyl substituted aza-BODIPY dye was employed as the core, due to its NIR absorbance and excellent optical properties, as well as easy modification at 2-position [38]. The probe **AZB-1** was then synthesized by introduction a conjugated, unsaturated ketone group at 2-position of aza-BODIPY core (Scheme 1). As shown in Fig. 1, the optical and photoacoustic properties were first investigated. All of them showed typical absorbance peaks around 660 nm. Upon excitation, the parent compound **4** gave an emission peak at 690 nm, and the precursor **5** showed a hyperchromatic emission at 650 nm. Both of compounds **4** and **5** displayed ignorable photoacoustic signals as expected (Fig. 1c). In contrast, the probe **AZB-1** showed almost no fluorescence, but with a strong photoacoustic signal. It is believed that the strong ICT effect occurred between the parent core and the conjugated α,β-unsaturated ketone group, relaxed the excited energy through a non-radiative pathway, resulting in switching its fluorescence into photoacoustic signal. Once reacting with $ONOO^-$, the double bond

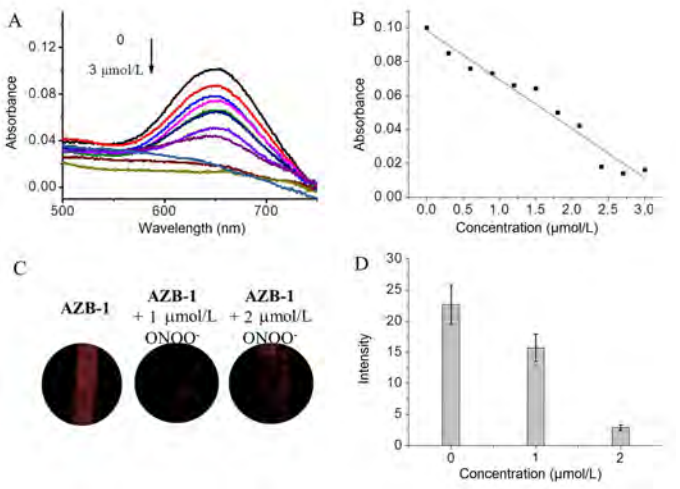

Fig. 2. (A) Absorption spectra of **AZB-1** probe after reaction with different concentrations of $ONOO^-$. (B) Absorption value of probe **AZB-1** at 660 nm after reaction with different concentrations of $ONOO^-$. (C) Photoacoustic signal of **AZB-1** reacting with different concentrations of $ONOO^-$. (D) Photoacoustic signal value of **AZB-1** reacting with different concentrations of $ONOO^-$. The excitation wavelengths were all at 660 nm.

could be oxidized, breaking the extending conjugated system, leading a turn-off photoacoustic response. These results indicated that the design strategy of photoacoustic probe could be realized by modifying aza-BODIPY with an election withdrawing group.

The solubility and aggregation behaviors of **AZB-1** were firstly examined. As showed in Figs. S1-S3 (Supporting information), **AZB-1** features a typical dose-dependent aggregation behavior in aqueous solutions due to its hydrophobic nature. The absorption intensity of the probe varies with the ratio of PBS buffer solution. **AZB-1** showed a stable response to $ONOO^-$ in a mixture aqueous solution (PBS:DMSO = 1:1) under the concentration of 3 μmol/L. In addition, we tried to increase the solubility by preparing nanoparticles. As showed in Fig. S4 (Supporting information), probe **AZB-1-F127** was assembled by the amphiphilic polyether F127 and formed a uniformed nanoparticle with an average diameter of 200 nm. However, the nanoparticles **AZB-1-F127** showed ignorable response after the reaction with $ONOO^-$. The results indicated that the polyether-coated probe cannot react with the $ONOO^-$, which may be because the $ONOO^-$ could not break through the outer polyether to enter the interior of the nanoparticle. Therefore, the subsequent tests were performed in mixture aqueous solution with **AZB-1**.

The response of **AZB-1** to $ONOO^-$ was then launched. As shown in the Fig. 2, in a mixture aqueous solution (DMSO:PBS = 1:1), the absorption intensity of the probe **AZB-1** at 660 nm gradually decreases with the increase of the concentration of $ONOO^-$, and the decrease of the absorption value has a good linear relationship with the concentration of $ONOO^-$. Meanwhile, the value of photoacoustic signal at 660 nm was significantly reduced, after the addition of $ONOO^-$ with different concentrations. These data indicated that this probe could detect $ONOO^-$ in solution by a photoacoustic way. In addition, the photoacoustic signal value of the probe **AZB-1** reduced obviously over the change of the concentration of $ONOO^-$, even 2 μmol/L $ONOO^-$ has quenched the photoacoustic signal.

The proposed sensing mechanism was documented in Scheme 2. According to the absorbance spectra (Figs. 2A and 1A), the product of **AZB-1** with $ONOO^-$ showed similar absorbance peak with compound **5**. Consequently, we assumed that the double bond of α,β-unsaturated ketone group could be readily oxidized, resulting in the quenching the photoacoustic signal. To confirm this proposed reaction mechanism, high resolution mass

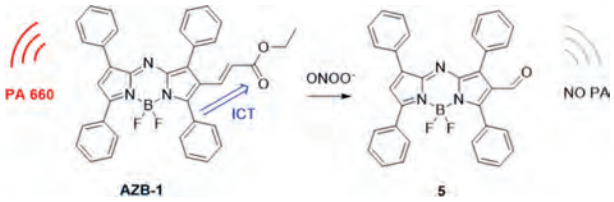

Scheme 2. Design concept and structures of **AZB-1** and **5**.

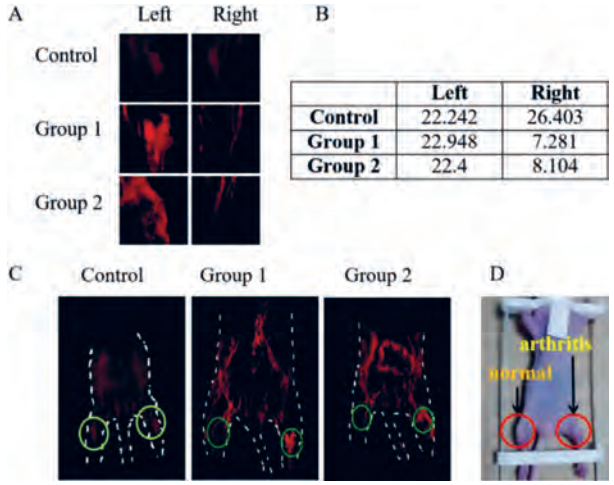

	Left	Right
Control	22.242	26.403
Group 1	22.948	7.281
Group 2	22.4	8.104

Fig. 3. (A) Photoacoustic imaging of left and right limbs of mice in control group and experimental group. The mice in the control group were injected with normal saline, while the mice in the experimental group had arthritis in the right limb and normal left limb. (B) Photoacoustic signal values of left and right limbs of mice in control group and experimental group. (C) Photoacoustic signal images of the whole body of mice in control group and experimental group. (D) Photograph of the experimental group mice (excitation wavelength is 660 nm).

spectra were used to investigate oxidation of **AZB-1** by $ONOO^-$. When 10 equiv. of $ONOO^-$ was added to the solution of **AZB-1**, a peak corresponding to $[\mathbf{5}-H]^-$ (Fig. S7 in Supporting information) appeared at *m/z* 566.8860, demonstrating that the compound **5** was generated.

Based on abovementioned data, we further investigated the actual application of **AZB-1** for photoacoustic imaging of $ONOO^-$ *in vivo*. All animal experiments were approved by the Institutional Animal Ethics Committee at Qingdao University, and the experiments were performed in compliance with the Care and Use of Laboratory Animal of Qingdao University. BALB/c nude mice (4–5 weeks) were used for establishment of mouse rheumatoid arthritis models by injecting λ-carrageenan (5 mg/mL, 50 μL in PBS) into the right hind limbs of mice. The left limbs were injected with normal saline (50 μL) as control. Four hours later, the right leg of the experimental mice was found to be arthritic and inflamed. It is known from previous reports that arthritis causes a rapid increase in the concentration of $ONOO^-$ [39]. Photoacoustic imaging was performed after intravenous injection of **AZB-1**. As shown in Fig. 3, there was no significant difference in photoacoustic signal values between the left and right limbs of the control group. But the photoacoustic signal of the right limb was significantly reduced in comparison with that of the left limb. These data demonstrated that probe **AZB-1** can be used as a reliable and high-resolution imaging tool for the detection of $ONOO^-$ variations in mice.

To conclude, we have developed a new photoacoustic probe **AZB-1**, which exhibits good sensitivity in monitoring $ONOO^-$ oxidation under solution and living mice. The fluorescence signal of the probe itself is very weak, but it has a very strong photoacoustic signal. When it reacted with $ONOO^-$ in solution system, the value of photoacoustic signal is significantly reduced. The same phenomenon can also be verified *in vivo*. When the probe was injected into mice, the photoacoustic signal of the right arthritis limb is very weak, while the photoacoustic signal of the left normal limb was obvious. The value of the photoacoustic signal of the left limb is about 3 times than that of the right limb. The results demonstrated the probe **AZB-1** can be used to detect $ONOO^-$ *in vivo*. Wisely utilized this strategy may serve as powerful platforms for the preparation of novel PA chemosensors in the future.

Declaration of competing interest

The authors declared that they have no conflicts of interest to this work.

Acknowledgments

Dr. Xin Zhou acknowledged the National Natural Science Foundation of China (Nos. 21662037, 21762045, 21911540466), Shandong Provincial Natural Science Foundation (No. ZR2019YQ12), China Postdoctoral Science Foundation (No. 219M652306), and Taishan Scholar Project (No. tsqn 201812049) for supporting this work. This research was also supported through the Basic Science Research Program of the National Research Foundation of Korea (NRF) funded by the Ministry of Education (No. 2017R1A6A3A04004954) to S. Lee.

Supplementary materials

Supplementary material associated with this article can be found, in the online version, at doi:10.1016/j.cclet.2021.05.048.

References

[1] F.J. Corpas, J.B. Barroso, Ann. Bot. 113 (2014) 87–96.
[2] H. Li, X. Li, X. Wu, W. Shi, H. Ma, Anal. Chem. 89 (2017) 5519–5525.
[3] J. Liu, Y. Dong, Y. Ma, et al., Nanoscale 10 (2018) 13589–13598.
[4] Y. Deng, G. Feng, Anal. Chem. 92 (2020) 14667–14675.
[5] J.H.M. Tsai, J.G. Harrison, J.C. Martin, et al., J. Am. Chem. Soc. 116 (1994) 4115–4116.
[6] G. Ferrer-Sueta, R. Radi, ACS Chem. Biol. 4 (2009) 161–177.
[7] C. Ducrocq, B. Blanchard, B. Pignatellib, H. Ohshima, Cell. Mol. Life Sci. 55 (1999) 1068–1077.
[8] Y. Li, X. Xie, X. Yang, et al., Chem. Sci. 8 (2017) 4006–4011.
[9] P. Pacher, J.S. Beckman, L. Liaudet, Physiol. Rev. 87 (2007) 315–424.
[10] T. Sawa, M.H. Zaki, T. Okamoto, et al., Nat. Chem. Biol. 3 (2007) 727–735.
[11] T. Koppal, J. Drake, S. Yatin, et al., J. Neurochem. 72 (1999) 310–317.
[12] D. Lee, C.S. Lim, G. Ko, et al., Anal. Chem. 90 (2018) 9347–9352.
[13] V.L. Dawson, T.M. Dawson, J. Chem. Neuroanat. 10 (1996) 179–190.
[14] T. Franc, S. Salman-Tabcheh, M.C. Guérin, J. Torreilles, Res. Rev. 30 (1999) 153–163.
[15] S. Wang, L. Chen, P. Jangili, et al., Coord. Chem. Rev. 374 (2018) 36–54.
[16] B. Li, Z. He, H. Zhou, H. Zhang, T. Cheng, Chin. Chem. Lett. 28 (2017) 1929–1934.
[17] X. Li, X. Gao, W. Shi, H. Ma, Chem. Rev. 114 (2014) 590–659.
[18] J.F. Zhang, Y. Zhou, J. Yoon, J.S. Kim, Chem. Soc. Rev. 40 (2011) 3416–3429.
[19] X. Chen, X. Tian, I. Shin, J. Yoon, Chem. Soc. Rev. 40 (2011) 4783–4804.
[20] J. Lu, Y. Song, W. Shi, X. Li, H. Ma, Sens. Actuators B: Chem. 161 (2012) 615–620.
[21] H. Maeda, H. Matsuno, M. Ushida, et al., Angew. Chem. Int. Ed. 44 (2005) 2922–2925.
[22] C. Yin, F. Huo, J. Zhang, et al., Chem. Soc. Rev. 42 (2013) 6032–6059.
[23] M. Xu, L.V. Wang, Rev. Sci. Instrum. 77 (2006) 041101.
[24] Q. Fu, R. Zhu, J. Song, H. Yang, X. Chen, Adv. Mater. 31 (2019) 1805875.
[25] L.V. Wang, Nat. Photonics 3 (2009) 503–509.
[26] J. Weber, P.C. Beard, S.E. Bohndiek, Nat. Methods 13 (2016) 639–650.
[27] K.J. Cash, C. Li, J. Xia, L.V. Wang, H.A. Clark, ACS Nano 9 (2015) 1692–1698.
[28] P. Beard, Interface Focus 1 (2011) 602–631.
[29] S. Mallidi, G.P. Luke, S. Emelianov, Trends Biotechnol. 29 (2011) 213–221.
[30] J. Jo, C. Tian, G. Xu, et al., Photoacoustics 12 (2018) 82–89.
[31] H. Li, P. Zhang, L.P. Smaga, R.A. Hoffman, J. Chan, J. Am. Chem. Soc. 137 (2015) 15628–15631.
[32] Y. Liu, S. Wang, Y. Ma, et al., Adv. Mater. 29 (2017) 1606129.
[33] X. Li, Y. Tang, J. Li, et al., Chem. Commun. 55 (2019) 5934–5937.

[34] J. Zheng, Q. Zeng, R. Zhang, D. Xing, T. Zhang, J. Am. Chem. Soc. 141 (2019) 19226–19230.
[35] C.J. Reinhardt, E.Y. Zhou, M.D. Jorgensen, G. Partipilo, J. Chan, J. Am. Chem. Soc. 140 (2018) 1011–1018.
[36] J. Zhang, X. Zhen, J. Zeng, K. Pu, Anal. Chem. 90 (2018) 9301–9307.
[37] X. Qin, F. Li, Y. Zhang, et al., Anal. Chem. 90 (2018) 9381–9385.
[38] W. Zhao, E.M. Carreira, Angew. Chem. Int. Ed. 44 (2005) 1677–1679.
[39] A.H. Panchal, N.J. Patel, N.G. Patel, et al., Pharma. Sci. Monit. 1 (2010) 79–94.